Real-time Identification and Quantification of Apple Scab on Fruit in Preharvest and Postharvest Conditions Using YOLOv11: A Deep Learning Approach

Fernanda Leiva

Fernanda.leiva@agroscope.admin.ch

Agroscope c/o DLZ FI EFD

Severine Gabioud Rebeaud

Agroscope c/o DLZ FI EFD

Danilo Christen

Agroscope c/o DLZ FI EFD

Research Article

Keywords: apple scab (AS), Venturia inaequalis, apple, fruits, deep learning, YOLO models, object segmentation, disease quantification, image analysis, fruit grading, machine learning

Posted Date: July 21st, 2025

DOI: https://doi.org/10.21203/rs.3.rs-7010152/v1

Additional Declarations: No competing interests reported.

Version of Record: A version of this preprint was published at Plant Methods on February 22nd, 2026.
See the published version at https://doi.org/10.1186/s13007-026-01508-7.

Real-time Identification and Quantification of Apple Scab on Fruit in Preharvest and Postharvest Conditions Using YOLOv11: A Deep Learning Approach

Fernanda Leiva*, Severine Gabioud Rebeaud, and Danilo Christen

Institute for Plant Production Systems, Agroscope, Route des Eterpys 18,

1964 Conthey, Switzerland.

Abstract

Background: Apple scab (AS), caused by the fungal pathogen *Venturia inaequalis*, is a major disease of apple that manifests as lesions on leaves and fruits. It significantly reduces fruit quality and yield, leading to substantial economic losses. Traditional AS assessment relies on visual scoring, which is labor-intensive, subjective, and poorly reproducible. This study proposes a deep learning-based framework to overcome these limitations and to enable an accurate, scalable AS phenotyping approach.

Results: Deep learning techniques were employed for the object detection and segmentation of AS symptoms in apple fruits. A two-stage fine-tuning process using the YOLO foundation model (YOLOv11) was applied to color images collected under orchard and laboratory conditions. The first model achieved over 90% precision in detecting apples, while the second achieved 78% precision in identifying and quantifying AS lesions. The YOLO-based architecture supports the real-time processing of both images and video streams, enabling rapid in situ evaluation. Despite challenges such as variable lighting, shading, and symptom heterogeneity across developmental stages, the model's performance was enhanced through extensive data augmentation, a diverse image dataset, and the use of high-resolution (840 × 840 pixels) training images, which improved detection of fine-scale features by 40% . Compared to manual scoring, this method is significantly faster, more objective, and more reproducible.

Conclusion: These results demonstrate the strong potential of the proposed deep learning-based approach as a robust and scalable tool for automated AS phenotyping. By improving the precision and efficiency of disease assessments in both controlled and field environments, this framework effectively supports apple grading assessments and accelerates breeding efforts aimed at identifying AS-resistant

genotypes. Moreover, it establishes a solid foundation for broader applications in real-time plant disease monitoring and the future integration of additional apple diseases.

Keywords

apple scab (AS), *Venturia inaequalis*, apple, fruits, deep learning, YOLO models, object segmentation, disease quantification, image analysis, fruit grading, machine learning

Background

Apple (*Malus domestica* Borkh), a temperate fruit tree native to Central Asia, is one of the most widely cultivated and economically valuable fruit crops worldwide. Annual global production of apple exceeds 86 million tons, making the fruit one of the major components of horticultural systems and a key source of dietary nutrients and income for millions of growers [1, 2]. Due to its sensory appeal as well as its nutritional and phytochemical richness, apple is the second most consumed fruit globally after banana [3], contributing significantly to human health by providing dietary fiber, antioxidants, and polyphenols [4, 5]. Apples are cultivated across more than 100 countries, spanning diverse climatic zones, owing to their extensive genotypic and phenotypic diversity [1]. This adaptability, as well as the broad production area, explains the large number of breeding initiatives aimed at improving resilience to biotic and abiotic stresses. Furthermore, breeding efforts increasingly focus on consumer-driven traits, such as flavor complexity, texture, and nutritional composition, reflecting the evolving demands of fresh and processed food markets [6].

Organic agriculture has emerged as a promising, yet debated, approach to improving the sustainability of modern food systems [7]. The approach is characterized by the avoidance of synthetic fertilizers and pesticides, the promotion of crop rotations, and an emphasis on soil health and closed nutrient cycles [8, 9]. It offers tangible environmental benefits across multiple indicators, including enhanced biodiversity, improved soil structure, and reduced chemical runoff [10]. These advantages have prompted growing consumer and policy interest in organically produced fruits, including apples. However, meeting the growing societal demand for the reduced use of synthetic pesticides has made

53 apple production increasingly challenging, primarily due to susceptibility to biotic stresses [11]. One of
54 the most significant threats is apple scab (AS), caused by the ascomycete fungus *Venturia inaequalis*
55 (Cooke) G. Winter, which severely compromises fruit quality by inducing lesions and cracking. This leads
56 to considerable economic losses, reduced yields, and an increased risk of mycotoxin contamination
57 during storage [12, 13].
58 In Switzerland, AS poses a persistent challenge, particularly driven by the country's humid and
59 temperate climate, which favors the proliferation of *V. inaequalis* and leads to recurrent annual
60 epidemics [12, 14]. Swiss orchards, especially in organic farming, adopt alternative strategies for
61 managing AS [15]. These approaches include cultural practices, such as pruning to improve air
62 circulation, sanitation methods to reduce pathogen inoculum, and the application of approved organic
63 fungicides, including sulfur-based products and plant-based extracts [16, 17]. However, assessing
64 susceptibility to AS presents considerable challenges, especially within genetic resource collections and
65 experimental orchards. For many years, apple breeders have introduced genes derived from wild apples
66 in new varieties that exhibit qualitative AS resistance. This qualitative resistance, controlled by a single
67 gene, is easy to identify through molecular methods [18-20]. The most well-known example of
68 qualitative resistance is Rvi6 (formerly Vf), widely used in apple breeding but increasingly overcome by
69 virulent Venturia inaequalis races [21, 22]. Other Rvi genes (e.g., Rvi1, Rvi2, Rvi4) also provide
70 qualitative resistance, and breeders aim to "pyramid" multiple Rvi genes for improved durability [23,
71 24]. However, resistance to AS also involves quantitative traits governed by multiple genes, making
72 assessments particularly time-consuming and challenging both in orchard and post-harvest settings.
73 The complexity and labor-intensive nature of accurately evaluating quantitative resistance highlight the
74 need for improved, efficient, and non-invasive diagnostic techniques that could enhance precision in
75 disease management strategies and in assessing genetic resources and varieties.
76 To address this challenge, recent research has increasingly focused on the integration of digital
77 phenotyping with deep learning (DL) approaches, particularly convolutional neural networks (CNNs).
78 These approaches offer rapid, non-destructive, high-throughput detection and quantification of plant

79 diseases, demonstrating significant accuracy and robustness in autonomously identifying disease-
80 specific visual features with minimal human intervention [25]. Some examples of CNN-based methods
81 applied for AS detection are presented in a study by Kodors et al. [26], who achieved an accuracy of
82 85% using a VGG-16 model, and by Patidar and Chakravorty [27], who demonstrated a lightweight CNN
83 capable of 95% accuracy for classifying common apple diseases.
84 Advanced models in object detection, such as you only look once (YOLO) algorithms [28], are known for
85 their speed and accuracy in real-time detection tasks. Unlike region-based approaches that process
86 portions of the image sequentially, YOLO models analyze the entire image in a single pass, drastically
87 reducing detection time while preserving high accuracy. These characteristics make YOLO-based
88 models highly suitable for in-field agricultural applications, including disease identification under
89 variable lighting and background conditions [29]. In the context of AS detection, YOLO-based models
90 (YOLOv5 and YOLOv7) have demonstrated robust performance, with successful applications under
91 diverse environmental conditions and across different plant organs, including leaves and fruits [30, 31].
92 However, such approaches typically emphasize binary classification, such as healthy versus unhealthy,
93 without addressing the assessment of symptom severity, which is critical for effective disease
94 management and commercial grading.
95 Furthermore, commercial methods for apple disease evaluation rely on sophisticated and often
96 expensive sorting machines equipped with advanced camera systems [32]. These systems can
97 accurately classify apples based on surface disorders, including AS lesions. Nevertheless, their high cost
98 limits accessibility, especially for smaller or organic producers. Moreover, such systems typically do not
99 provide a single severity disease assessment and miss the opportunity for storage disease management
100 interventions, such as decision support systems for postharvest treatments (e.g., heat water
101 treatments) or for early sale windows of some apple batches.
102 Methods for detecting AS presence and assessing severity levels through CNN-based models were first
103 presented by Rath [33], who fine-tuned a ResNet34 model, achieving a validation accuracy of 94% on a
104 dataset comprising images of healthy and scab-infected apples. Similarly, Kavya et al. [34] compared

multiple CNN architectures (including VGG-16, ResNet-50, and MobileNet). The MobileNet model achieved the highest accuracy at 98% in detecting and quantifying AS severity. Despite their promising results in both studies, the image-based detection methods are limited to controlled environments or to datasets with uniform lighting conditions, which restricts their effectiveness under varied or adverse environmental conditions commonly encountered in orchard settings.

Hence, improving AS detection methods must address two key production stages: preharvest and postharvest. Preharvest improvements involve enhancing the selection of resistant cultivars by improving the early detection and accurate classification of AS symptoms, thus benefiting breeding programs and targeted disease management strategies. Postharvest advancements focus on developing methods to monitor symptom progression during storage for the early detection of scab progression and refining sorting processes to accurately assess AS severity, an operation that cannot be achieved with a sorting machine [35]. Although minor scab lesions are accepted to some extent in organic apple production, particularly for apples sold as table fruit in Switzerland [36], this limited tolerance underscores the importance of accurate severity-based grading and the need for reliable assessment methods to ensure proper assessment and marketability.

To address these limitations, this study proposes a lightweight model capable of detecting and quantifying AS severity under various environmental conditions, including both orchard and laboratory settings (postharvest). A YOLO segmentation model (YOLOv11-seg) was trained on a comprehensive image dataset containing healthy and scab-infected apples, with performance enhanced through data augmentation techniques. This efficient, nondestructive tool enables real-time evaluation using either images or video, leveraging the speed and versatility of YOLO-based architectures. As a result, it can significantly improve disease monitoring and apple grading accuracy, contributing meaningfully to more sustainable and precise disease management practices.

Materials and methods

Image acquisition

Images were captured using a Sony RX1-RII camera with a sonar lens of 20–35 mm and a resolution of 42.4 megapixels to capture high-quality images affected by AS. The camera was mounted on a telescope background system (Walimex Telescope 1, 2, or 3 meters high) with a multifunctional super clamp. The images in baskets were taken from the top of the telescope and the images in the orchards from halfway down of the telescope in both cases approximately 1 m from the target. The camera was powered with a battery bank of 16 V, which was connected to a step-down voltage transformer to provide the corresponding 5 V to the camera. Images were taken from different angles at different points of the day to create variability in the dataset and were stored in JPEG format with a pixel resolution of 3984 × 2656. An overview of the imaging setup under both indoor and outdoor conditions is presented in Figure 1. Although a multispectral camera was initially evaluated, the information captured from apple fruits using multispectral imaging proved less informative than that obtained from standard RGB images.

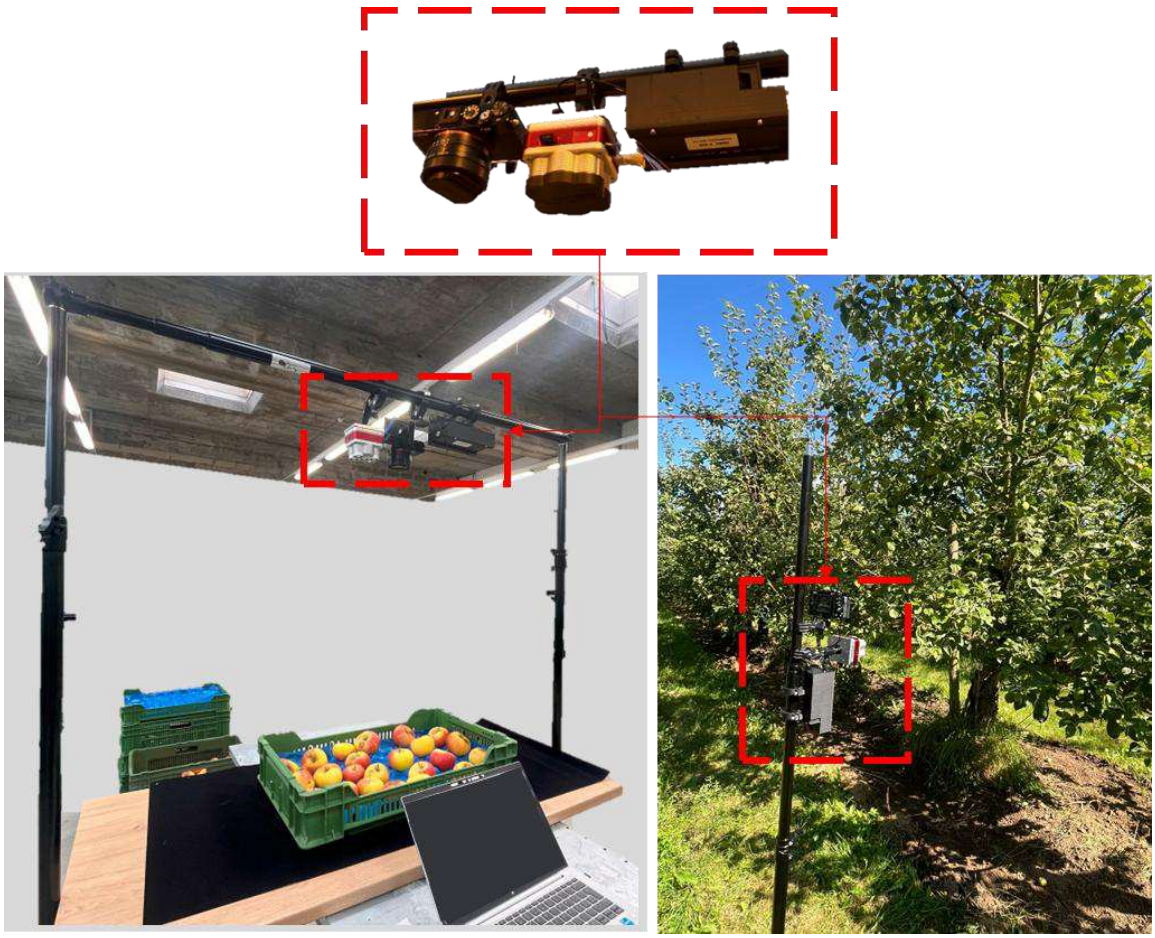

144 Figure 1. Schematic representation of the image acquisition setup used under controlled (indoor) and
145 orchard (outdoor) conditions. The left panel shows the setup in laboratory environments; the right
146 panel shows deployment in orchard settings. The red boxes denote the position and configuration of
147 the imaging equipment.
148
149 *Plant material and database*
150 The image dataset collection focused on apple samples highly infected with AS collected from two
151 different sources. The first source was organically managed orchards located at the Research Institute
152 of Organic Agriculture (FiBL) in Frick, Switzerland, 350 m above sea level, with images captured under
153 both real field and postharvest conditions. The second source of the infected apples was the Swiss
154 Confederation's center for agricultural research Agroscope in Conthey, Switzerland, 504 m above sea
155 level, using postharvest apple fruits under storage conditions, from several organic farms near the
156 research center. The timing of symptom appearance on fruits is highly dependent on when the infection
157 occurs and the environmental conditions from spring and continue to develop throughout the growing
158 season. Where, daily minimum and maximum temperatures range from 12°C to 22°C ± 2°C, with
159 humidity varying between 65% and 70% (agrometeo.ch). The apples in the postharvest from the second
160 source were stored under controlled storage conditions typically used for maintaining postharvest fruit
161 quality. These conditions included temperatures ranging from 0°C to 4°C, with relative humidity
162 maintained at approximately 90–95%, which are standard parameters for reducing metabolic activity
163 and delaying the development of storage-related disorders. Prior to imaging, the apples were taken
164 from the storage room and left at ambient room temperature for approximately 1 h. This
165 acclimatization step was critical to minimizing surface condensation and humidity-related artifacts that
166 could interfere with image quality and analysis. Apple images were captured at multiple time points
167 throughout the storage trial to monitor symptom progression over time. This approach enabled the
168 documentation of dynamic changes in visual appearance due to storage-related physiological or
169 pathological developments, supporting both early detection efforts and severity assessments during

postharvest evaluations. In addition, for the robustness of the model, several publicly available labeled and unlabeled datasets of apples with and without AS, samples with other non-identified lesions (other diseases or mechanical damages) from Roboflow [37], and images provided by Kodors et al. [26] in Kaggle were included. An example of the variability of the dataset is shown in Figure 2.

Figure 2. Representative examples from the image dataset. (A) Images captured in orchard conditions: the top-left panel shows a tree with healthy fruit (sourced from an online database), and the top-right panel shows infected fruits, with the latter captured at close range. (B) Images obtained under laboratory conditions during postharvest and storage: the bottom-left panel displays infected fruits, and the bottom-right panel shows healthy fruits.

Scab phenotyping and visual scoring

AS phenotyping and visual scoring are traditionally performed at multiple stages, including in orchards, immediately postharvest, and during storage. In orchard conditions, visual assessments are conducted by trained evaluators who inspect a representative sample of fruits per tree using standardized scales [38] (Table 1). Postharvest phenotyping is carried out in controlled indoor environments, where each fruit is manually rotated to allow for a thorough surface examination. Based on the presence, number,

and size of the lesions, fruits are either selected for juice processing or forwarded for storage evaluation. During storage trials, fruits are periodically inspected to assess overall health and monitor disease progression. Each fruit is evaluated for lesion size, number, and distribution, with visual differentiation performed to distinguish AS lesions from other storage-related disorders, such as lenticel breakdown or fruit rots.

Table 1 Evaluation scale for scab severity (adapted from [38])

Class	Symptoms	Proportion affected (%)	
0	NA	-	NA
1	No visible lesions	0%	
2	One or very few lesions detectable.	0–1 %	
3	Immediately apparent lesions	1–5 %	
4	Intermediate	x	
5	Numerous lesions widespread	± 25 %	

6	Intermediate	x	
7	Badly infected by multiple lesions	± 50 %	
8	Intermediate	± 75 %	
9	Completely affected (nearly all)	> 90 %	

194

195 *Image and data processing*

196 Images were manually annotated in two stages using two free software. First, “Anylabeling” software
197 incorporating artificial intelligence (AI) was used, employing the Segment Anything Model (SAM) to
198 facilitate annotations of big objects, specifically, individual apples categorized as “apples.” In the second
199 stage, LabelMe software was used to annotate small objects, specifically the lesions associated with AS
200 disease and other non-identified disorders. These were categorized as “scab” and “disease,”
201 respectively. All annotations were generated in JSON format for LabelMe and subsequently converted
202 into YOLO format using the “labelme2yolo” tool to meet the input requirements of the YOLO model for
203 image segmentation.
204 To enhance model generalization and robustness, data augmentation techniques were applied using
205 the OpenCV package (Open-Source Computer Vision Library), including horizontally and/or vertically
206 flip, translation, zooming, rotation, and their combinations. These transformations expanded the
207 dataset to a total of 42000 images. The images were then categorized into three datasets based on

their source: (1) images obtained from various online databases (37,699 images), (2) images captured under field conditions (2,043 images), and (3) images acquired in laboratory settings (1,918 images).

Modeling

Hardware system

The models were trained on a Lenovo ThinkPad P15 computer with an Intel Core i9 processor, an NVIDIA Quadro RTX 5000 Max-Q GPU (16 GB), and the Ubuntu 22.04 64-bit operating system.

Model selection and training strategy

To ensure the optimal performance of the object detection and segmentation models, several preliminary tests and iterative refinements were conducted before finalizing the training pipeline. Initially, YOLOv8 was selected due to its strong balance between speed and accuracy in real-time segmentation tasks. At the time, it was one of the most widely supported models for segmentation. With the release of YOLOv11, the model architecture was updated due to its enhanced support for custom anchor generation, an important feature for detecting small and irregularly shaped objects, such as scab lesions. YOLOv11 divides the input image into a grid of S × S cells, following the same approach as previous YOLO versions. Each cell is responsible for detecting objects whose centers fall within its boundaries. This grid-based strategy enables the model to predict bounding boxes and class probabilities in a single forward pass, thereby maintaining real-time detection capabilities. YOLOv11 directly predicts the center coordinates and dimensions of objects relative to each grid cell, which simplifies the detection process and reduces computational complexity, resulting in more efficient and accurate object detection [39]. An overview of this process is illustrated in Figure 3. In addition, Version 11 has an improved backbone, allowing detailed spatial features needed for segmentation, maintaining accuracy, and reducing computational time. The primary convolutional (Conv) block from previous versions is retained but is connected to the Cross Stage Partial with kernel size 2 (C3K2) after each iteration. The C3k2 block enhances the overall performance of the feature aggregation process, making it faster and more efficient. Additionally, the spatial pyramid pooling - fast (SPPF) block is connected to

the cross-stage partial with spatial attention (C2PSA) block. C2PSA improves spatial attention in feature maps, allowing the model to focus more effectively on specific areas of interest within the image. An overview of the YOLO11 architecture backbone is shown in Figure 4.

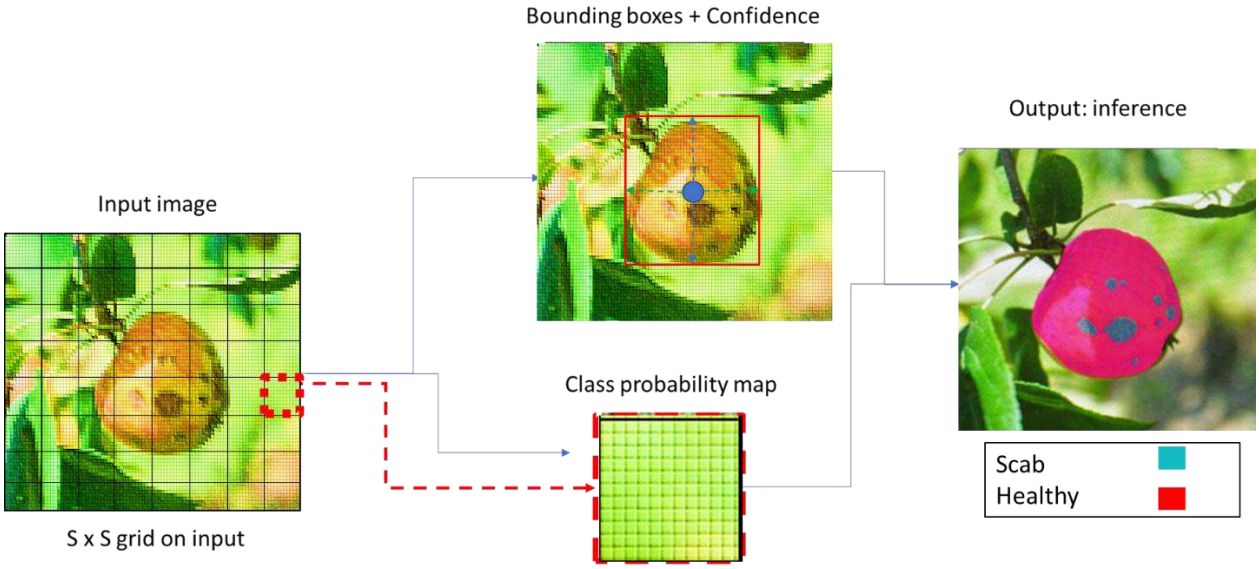

Figure 3. Model overview using an S x S grid and the free anchor object to produce the class probability and the final inference.

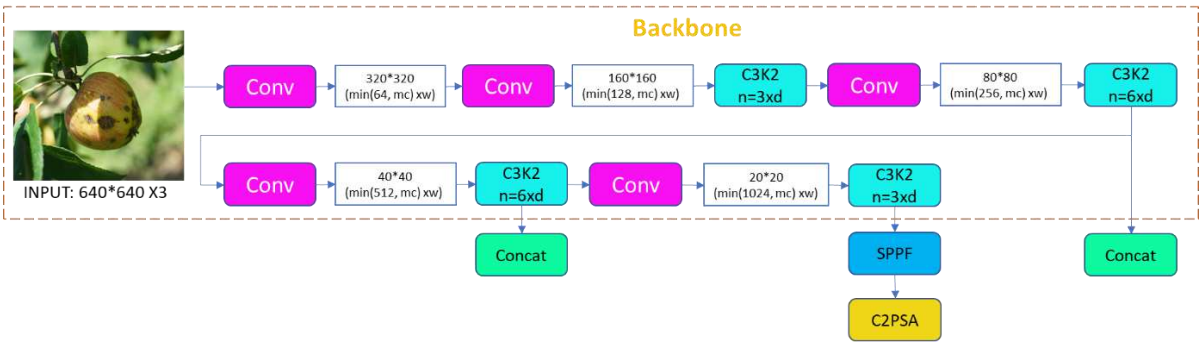

Figure 4. Schematic overview of the YOLO architecture. This illustration depicts the core components of the YOLO model framework, highlighting its end-to-end processing pipeline. Image adapted and recreated based on a visualization from Medium.com [39].

The annotation strategy underwent significant evolution. In the initial approach, apples were labeled as either "**healthy**" or "**unhealthy,**" with additional polygon annotations on unhealthy apples to denote specific disorders such as scab, general disease, or unknown defects. However, this method introduced

interpretability issues, as YOLO treats each class as an independent instance and lacks the capability to associate an apple with its internal disease regions. Consequently, early models trained using this labeling method struggled to distinguish between healthy and unhealthy apples reliably, often causing confusion during inference.

To address this, a two-step training approach was first attempted: (1) detecting apples and classifying them as healthy or unhealthy, and (2) fine-tuning the model to localize disease regions only on detected unhealthy apples. This yielded suboptimal results, prompting a re-evaluation of the labeling strategy. The revised approach unified all apples under a single "apple" class, while disease regions (e.g., scab, other diseases, and unknown disorders) were treated as separate classes. A key enhancement included label prioritization, where overlapping annotations were reordered to give precedence to scab regions, which is critical for the accurate segmentation of small lesions.

Despite this improvement, the initial experiments still showed low precision, particularly for scab detection. The datasets were then split based on environmental conditions (e.g., indoor vs. outdoor images), but false negatives persisted, particularly among the "unknown," "disease," and "background" classes. The ambiguous "unknown" category was ultimately removed, and all non-scab pathologies were grouped under a general "disease" label. This adjustment significantly improved precision, although performance remained below expectations.

To further enhance generalization, a staged training approach was adopted. The model was first trained on publicly available datasets with well-annotated disease labels to establish a strong baseline. It was then fine-tuned using the custom dataset collected in this study. However, this strategy also yielded results comparable to earlier tests, suggesting that data origin was not the primary limitation affecting performance.

The final training strategy employed a robust two-phase approach. In the first phase, the model was trained solely on images of healthy apples to learn general object features. Although YOLO already integrates this feature, the variability of cultivars and segmentation was improved, as were images taken under different lighting conditions. In the second phase, fine-tuning was performed on the full

dataset, including healthy, scab-affected, and diseased apples, using a reduced learning rate to preserve the first model results. Extensive hyperparameter tuning was performed to optimize model training, including adjustments to batch size, learning rate, and training duration, using the Ultralytics tuner, which identifies optimal values through weighted random mutations. To determine the optimal number of training epochs, multiple tests were conducted to identify the points of underfitting and overfitting. Finally, after several tests, the first model was trained for up to 100 epochs, with an early stopping mechanism based on a patience parameter set to 10 epochs. Thus, training was halted if no significant improvement in validation loss was observed over 10 consecutive epochs, thereby preventing unnecessary training and mitigating the risk of overfitting. For the other model, the number of epochs was set to 300 without patience, allowing an early stop if needed. In the case of batch size, the parameter that defines the number of images processed in one training iteration was set to 8. It is known that a larger batch size can improve training efficiency, but this requires more memory and may lead to less stable updates [40]. Additionally, during training, extra augmentations were applied to enhance model generalizability and reduce overfitting as variations of the HSV (hue, saturation, and value) color image representation. An overview of the processing chain is shown in Figure 5.

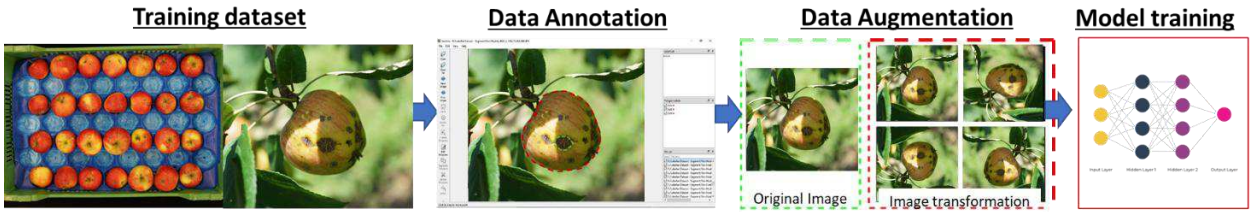

Figure 5. Workflow of the image processing pipeline for AS detection and quantification.

Model performance and disease assessment

To evaluate the model's performance, several standard metrics were used. Precision (P) assesses the model's ability to avoid false positives (Equation 1), while recall (R) measures its effectiveness in detecting all relevant instances of a class (Equation 2). Average precision (AP) combines both precision and recall into a single score (Equation 3). Mean average precision (mAP) computed at various

297 intersection over union (IoU) thresholds provides a comprehensive evaluation of localization accuracy
298 (Equation 4). Typically, an IoU threshold of 0.5 is used to determine whether an object is correctly
299 detected (acceptable performance), while a range of thresholds from 0.50 to 0.95 in 0.05 increments
300 offers a more nuanced assessment of the model's performance.

301 *Equation 1. Precision* $(P) = \frac{True\ positive}{True\ positive + False\ positive} x100\%$

302 *Equation 2. Recall* $(R) = \frac{True\ positive}{True\ positive + False\ Negative}\ x100\%$

303 *Equation 3. Average precision* $(AP) = \int_0^1 Precision(r)\ dr$

304 *Equation 4. Mean average precision* $(mAP) = \frac{1}{N}\sum_{i=1}^{N} AP_i$

305 A disease scoring assessment was performed based on the well-defined evaluation scale adapted from
306 Lateur and Populer in 1994 [38] (Table 1). Each apple was assigned an ID by checking the bounding box
307 overlap, and then the disease area per apple was computed (Equation 1Equation 5). The results were
308 obtained either for a single image or for a group of images and recorded in an Excel file.

309 *Equation 5. Percentage =* $\left(\frac{Disease\ Area}{Apple\ Area}\right) x\ 100$

310 ## Results

311 The first model, trained using images with healthy apples, achieved a mAP@50 of 97%, demonstrating
312 its ability to accurately identify apples under indoor and outdoor conditions. Additionally, the model
313 obtained mAP@50-95 for "all" classes of 0.94 for Box and 0.92 for mask, indicating that the predicted
314 bounding boxes and masks were very precisely aligned with the ground truth, as shown by the metric
315 results in Error! Reference source not found.. The second model, trained on images captured under
316 indoor postharvest and outdoor in orchards conditions, including apples with scab symptoms and
317 other disorders, achieved a mAP@50 of 89% for all the classes, specifically 75% for AS, confirming its
318 capability to effectively identify healthy from unhealthy apples, and scab like-lesions from other
319 defects (

320 Table 3).

321 *Table 2 Performance of the first model for apple identification (outdoor and indoor).*

Class	Images	Instances	Box				Mask			
			Precision	Recall	mAP 50	mAP 50-95	Precision	Recall	mAP 50	mAP 50-95
all	7226	19225	0.98	0.95	0.97	0.94	0.98	0.95	0.97	0.92
Apple	6482	8140	0.98	0.95	0.97	0.94	0.98	0.95	0.97	0.92

Table 3 Performance of the second model for apple disease identification (outdoor and indoor).

Class	Images	Instances	Box				Mask			
			Precision	Recall	mAP 50	mAP 50-95	Precision	Recall	mAP 50	mAP 50-95
all	6614	25498	0.93	0.89	0.89	0.83	0.84	0.89	0.88	0.79
apple	1130	1462	0.98	0.98	0.99	0.95	0.92	0.98	0.96	0.93
disease	2230	3738	0.97	0.91	0.94	0.85	0.96	0.96	0.94	0.78
scab	123	12366	0.85	0.78	0.75	0.70	0.64	0.75	0.75	0.68

The training and validation performance of the first YOLO model over approximately 100 epochs is shown in Figure , with the first graph presenting the training and validation performance of a YOLOv11 model trained solely in healthy apples. The losses for bounding box prediction, segmentation, and classification decreased steadily, indicating effective learning. The precision, recall, and mAP metrics for both bounding boxes and segmentation masks showed consistent improvement, suggesting that the model effectively detected and segmented healthy apples. Similarly, Figure 7 shows the results from training the model with both healthy and unhealthy apples (containing scab and other disorders), exhibiting a similar trend in decreasing losses and improving metrics. However, the model's performance on unhealthy apples, particularly those with scab lesions and other disorders, was slightly lower than on healthy apples. The precision and recall for bounding boxes and segmentation masks

improved but showed a small drop in mAP scores, indicating the added complexity of detecting and segmenting diseased apples. Nonetheless, the model still demonstrated solid performance in both object detection and segmentation tasks.

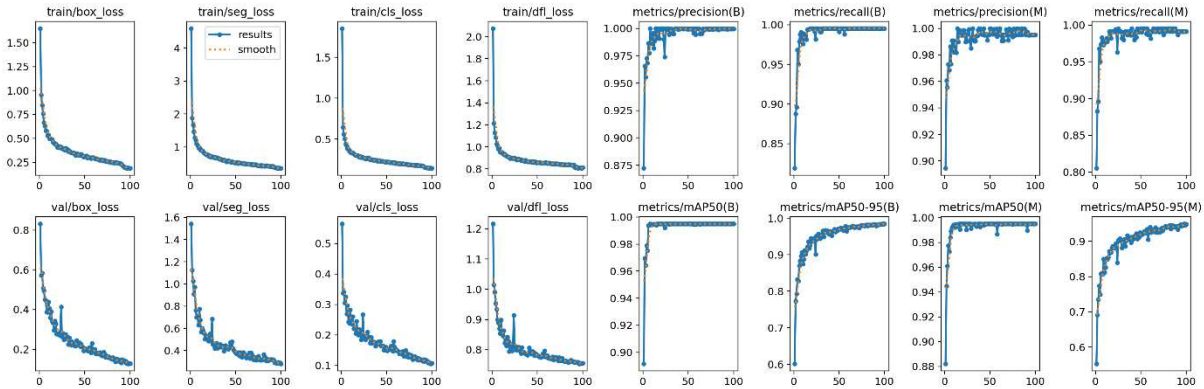

Figure 6. Training and validation performance of the first YOLO model over 100 epochs for healthy apple identification (outdoor and indoor).

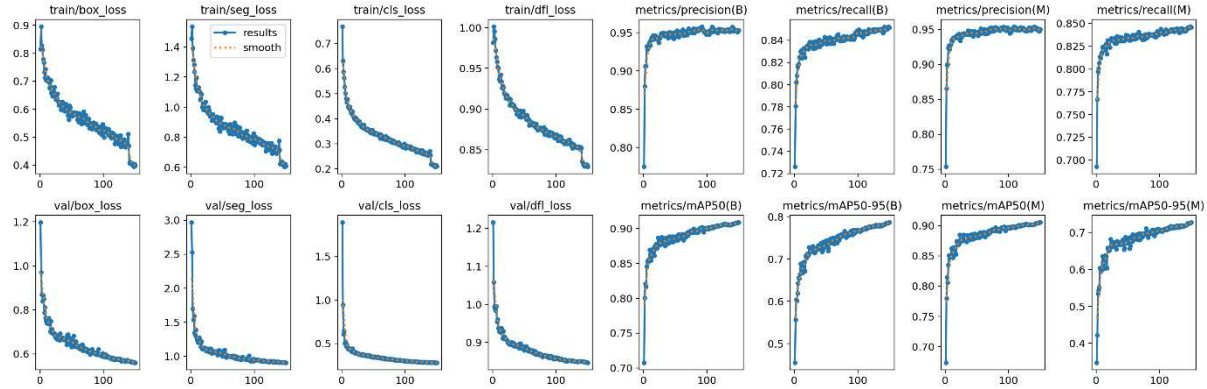

Figure 7. Training and validation performance of the fine-tuned YOLO model over 200 epochs for disease identification of healthy and unhealthy apples (outdoor and indoor).

The YOLO-based detection and segmentation model was then implemented in a pipeline to analyze scab disease severity. These preliminary results can be observed in Figure 8, with each image displaying the model's outputs, including object detection bounding boxes, segmentation masks, class labels (e.g., "apple"), and associated confidence scores. The detection process involved extracting bounding boxes

for each detected object, assigning a unique Apple ID, and calculating the proportion of diseased area relative to the total apple area. Disease severity was quantified using the scoring system, where severity scores ranged from 1 (healthy) to 9 (highly diseased) based on predefined percentage thresholds [38]. The results were automatically stored in an Excel file containing details such as Apple ID, classification, total apple area, disease-affected area, and computed disease percentage. Additionally, an output image was produced, displaying the Apple ID with the bounding box and its corresponding segmentation for clear and interpretable visualization (Figure 9). The proposed approach enhances the efficiency of automated fruit quality assessment while maintaining high interpretability and computational efficiency, making it suitable for real-time agricultural applications.

Figure 8. Use of the final model on images captured under various conditions: (A) predictions of healthy apples; (B) predictions of scab-infected apples. Images were sourced from both indoor (laboratory) and outdoor (orchard) environments.

A)

B)

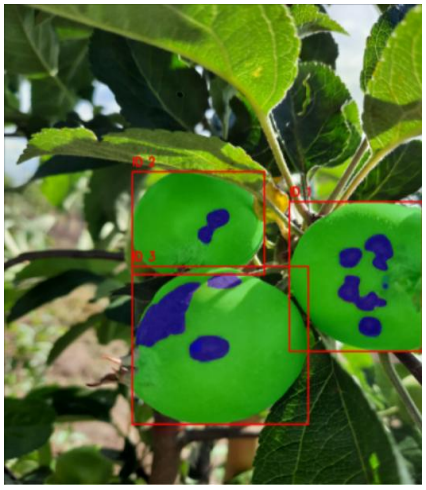

C)

```
Detected 3 apples and 8 marks.

Apple ID 1: Marks=4, Disease%=12.51%, Score=4
Apple ID 2: Marks=1, Disease%=4.57%, Score=3
Apple ID 3: Marks=3, Disease%=12.86%, Score=4
```

Figure 9. Examples of output data for AS identification and severity quantification: (A) original image of apples exhibiting scab symptoms, extracted from an openly available dataset [26]; (B) processed image displaying detection and segmentation results; (C) Output data, including scab severity scores.

Discussion

This study proposes an AI-based image processing method for detecting AS and assessing disease severity in apple fruit. To provide an effective solution, challenges in AS management strategies were evaluated by comparing conventional approaches with modern methodologies. Traditionally, scab management primarily relies on fungicide applications. However, this strategy is unsustainable and harmful to the environment and can lead to the development of fungicide-resistant pathogen strains with prolonged and repeated use [41, 42]. An alternative involves cultivating resistant apple varieties. Identifying resistant traits and genotypes has typically been conducted via visual assessments. However, resistance breeding poses its own set of challenges, particularly regarding the evaluation of quantitative resistance. Unlike qualitative resistance, typically governed by single, major resistance genes and identifiable through molecular markers, quantitative resistance is controlled by multiple

genes with small additive effects and strong interactions with environmental factors, making its assessment inherently complex and less consistent [43, 44]. The evaluation of such resistance often requires multi-year, multi-site field trials to capture variability in climate, pathogen pressure, and plant responses [18]. Visual scoring methods, although commonly used, are labor-intensive, subjective, and lack reproducibility, limiting their scalability and precision [45].

Recent quantitative trait locus (QTL) mapping studies have identified genomic regions associated with field resistance to scab, offering valuable tools for marker-assisted selection and a better understanding of the genetic architecture of resistance [46]. However, many of these loci provide partial resistance, which may reduce lesion size or delay symptom onset but not entirely prevent infection. The integration of image-based automated phenotyping systems could help overcome current limitations by improving the speed and objectivity of data collection. Overall, combining high-resolution phenotyping tools with molecular breeding approaches is essential for advancing the development of durable scab-resistant cultivars.

Recent advancements in DL and image processing techniques have shown significant potential in addressing phenotyping challenges. Among the most widely used state-of-the-art models for segmentation is Mask R-CNN, especially in detecting small objects [47]. Mask R-CNN has been employed for apple fruit disease diagnosis in different environments [48-50], demonstrating improved performance over traditional methods. Other high-performing segmentation models, such as SAM version 1 (SAM) and version 2 (SAM2), have also demonstrated excellent generalization and segmentation accuracy [51]. However, the fine-tuning process of both SAM and SAM2 is computationally demanding and resource-intensive, which does not facilitate real-time deployment.

The YOLO series from Ultralytics belongs to the most used and efficient DL models for real-time object detection. Although earlier YOLO versions struggled with detecting small objects [52, 53], the latest YOLOv11 model applied in this study addresses this limitation through an anchor-free detection mechanism adaptable to objects of varying sizes and shapes. Unlike the Mask R-CNN and SAM series, YOLO models offer superior real-time performance and fully automated instance segmentation with

406 minimal latency, making them practical for real-time and edge deployment. Additionally, YOLO is easily
407 fine-tuned to specific datasets, thereby improving domain-specific segmentation accuracy, a feature
408 limited in foundational models such as SAM.
409 In the domain of AS detection and severity assessment of apple fruits, various DL approaches using
410 YOLO architecture have been explored. For instance, a model named AppleScab was developed in 2023,
411 integrating the CARAFE architecture into YOLOv7 to enhance detection under varied lighting conditions.
412 Their model achieved a mean average precision ($maP_{0.5-0.95}$) of 64% and a detection time of 0.1752
413 seconds per image [54]. While this indicates strong performance in terms of speed, the reported speed
414 is dependent on multiple factors, including image resolution, system processor, and GPU capacity. In
415 their study, the authors utilized an NVIDIA GeForce RTX 3050, a GPU well-suited for light to moderate
416 DL workloads. As a result, the model was limited to smaller image datasets with an input size of 416 ×
417 416 pixels. This hardware configuration, particularly with larger models or higher-resolution images,
418 could impact scalability and generalizability in real-world applications. By contrast, the study presented
419 here demonstrated that processing a high-resolution image (1616 × 1080 pixels) takes approximately
420 0.6 s on the hardware settings mentioned in the materials section. This represents a significant trade-
421 off, given the substantial increase in image data.
422 Furthermore, unlike other studies that relied solely on controlled light conditions [26, 27], the proposed
423 method employs a robust two-step fine-tuning approach. This begins by training the pre-trained model
424 (YOLOv11-seg) offered by Ultralytics on our custom dataset, which encompasses different varieties of
425 healthy apples under different environmental conditions. The second fine-tuning step is to train the
426 resulting model on apples infected with disease symptoms (scab and others) under indoor and outdoor
427 conditions. The indoor dataset specifically addresses postharvest AS monitoring, focusing on storage
428 conditions in which latent symptoms progressively emerge, potentially affecting fruit quality and
429 marketability. By integrating AS detection capabilities into storage facilities, real-time monitoring
430 becomes feasible, informing decision-making regarding storage duration, fruit sorting, and fruit sale
431 periods. The outdoor dataset is intended to provide a tool for integration into automated orchard

monitoring systems, sorting lines, and postharvest storage management to enhance efficiency and minimize visual inspection reliance.

However, a notable limitation inherent to the 2D image acquisition setup used in this study is that the evaluation is performed only on one side of the apple at a time. This limitation increases the risk of misclassification, as lesions on the unscanned side may remain undetected, potentially classifying unhealthy apples as healthy. Addressing this challenge could involve multi-view imaging or the integration of the method with automated apple rotation and scanning systems, ensuring a comprehensive and accurate assessment of the entire fruit surface.

Despite this limitation, the practical application of DL models demonstrated in this study significantly contributes to precision agriculture, aligning well with previous research emphasizing the importance of accurate disease severity assessment [33, 34]. Future research should expand the dataset to encompass a broader range of apple varieties, environmental conditions, and disease progression stages to improve model generalization. Additionally, exploring hybrid models that combine indoor and outdoor datasets into a single adaptable system could further enhance robustness and accuracy. Incorporating explainable AI techniques might provide deeper insight into disease epidemiology and development, guiding researchers, warehouse operators, marketers, and growers toward more informed and effective management strategies.

Conclusions and future work

This study evaluated the performance of the YOLOv11 DL model for detecting AS and measuring AS severity on the surface of fruits under orchards and laboratory settings. By employing the object detection and segmentation model, a robust framework for scab phenotyping was developed that enables accurate, consistent, and rapid assessments. The model, trained on diverse image datasets, achieved a precision of 75%, demonstrating its potential for supporting the screening of AS apple genotypes and facilitating postharvest quality evaluation. By standardizing scab detection through AI phenotyping tools, this work contributes to building precision horticulture and breeding programs

focused on sustainable apple production. The proposed method reduces subjectivity scab scoring, improves reproducibility, and provides a scalable platform for use across varying production environments.

Future work should focus on deploying this system on edge-computing hardware, such as NVIDIA Jetson, for in-field, real-time monitoring, and extending its capabilities to detect multiple apple diseases, including lenticel rot. These efforts can enhance the practicality and relevance of AI-based phenotyping tools, ultimately accelerating the development of resilient apple cultivars and promoting data-driven decision-making in fruit production systems.

Abbreviations

AI: Artificial intelligence

AS: Apple scab

CNN: Convolutional neural network

DL: Deep learning

mAP: Mean average precision

ML: Machine learning

SAM: Segment anything model

YOLO: You only look once

Acknowledgments

The authors would like to acknowledge the contributions of the participants in this study: Sarah Boutillier, Clemence Boutry, Marie Cachat-Terrettaz, Samuel Köchli, Brhayan Liberato-Tafur, and Hans-Jakob Schärer.

Author contributions

D.C.: project planning and funding acquisition; S.D.: conceptualization, material acquisition, and review of disease identification; F.L.: experimentation, image collection, data labelling, data analysis, and manuscript writing. All authors assisted with revisions and corrections.

Funding

This project received funding from the European Union's Horizon Europe research and innovation program under grant agreement No. 101061028.

Data availability

This study analyzed a combination of publicly available datasets and data collected by the authors. To request the complete dataset, please email the corresponding author.

Corresponding author

Correspondence to Fernanda.leiva@agroscope.admin.ch.

Declarations

Ethics approval and consent to participate

Not applicable.

Consent for publication

All authors agreed to publish this manuscript.

References

1. FAO. Food, and Agriculture Organization of the United Nations. Rome, URL: http://faostat.fao.org, 2018. 403.
2. Hummer KE, Janick J. Rosaceae: taxonomy, economic importance, genomics. Genetics and Genomics of Rosaceae. 2009:1-17.
3. Hyun TK, Jang K-I. Apple as a source of dietary phytonutrients: an update on the potential health benefits of apple. EXCLI Journal. 2016;15:565.
4. Mierczak K, Garus-Pakowska A. An overview of apple varieties and the importance of apple consumption in the prevention of non-communicable diseases—a narrative review. Nutrients. 2024;16(19):3307.
5. Zhang Y, et al. Does an apple a day keep away diseases? Evidence and mechanism of action. Food Science & Nutrition. 2023;11(9):4926-47.
6. Migicovsky Z, et al. Genome to phenome mapping in apple using historical data. The Plant Genome. 2016;9(2):plantgenome2015.11.0113.
7. Foley JA, et al. Solutions for a cultivated planet. Nature. 2011;478(7369):337-42.

8. Seufert V, Ramankutty N, Foley JA. Comparing the yields of organic and conventional agriculture. Nature. 2012;485(7397):229-32.
9. Tuomisto HL, et al. Does organic farming reduce environmental impacts?–a meta-analysis of European research. Journal of environmental Management. 2012:112: 309-20.
10. Muller A, et al. Strategies for feeding the world more sustainably with organic agriculture. Nature Communications, 2017;8(1):1290.
11. Vasylieva N, Harvey J. Production and trade patterns in the world apple market. Innovative Marketing. 2021;17(1):16.
12. Belete T, Boyraz N. Critical review on apple scab (Venturia inaequalis) biology, epidemiology, economic importance, management and defense mechanisms to the causal agent. J. Plant Physiol. Pathol. 2017;5(2):2.
13. MacHardy WE, Apple scab: biology, epidemiology, and management. 1996.
14. Zachmann L, McCallum C, Finger R. Farm-level data on production systems, farmer- and farm characteristics of apple growers in Switzerland. Data in Brief. 2023;50:109531.
15. Mathis M, et al. Comparison of exemplary crop protection strategies in Swiss apple production: multi-criteria assessment of pesticide use, ecotoxicological risks, environmental and economic impacts. Sustainable Production and Consumption. 2022;31:512-28.
16. Carisse O, Dewdney M. A review of non-fungicidal approaches for the control of apple scab. Phytoprotection. 2002;83(1):1-29.
17. Didelot F, et al. Sustainable management of scab control through the integration of apple resistant cultivars in a low-fungicide input system. Agriculture, Ecosystems & Environment, 2016;217:41-48.
18. Papp D, et al. Field apple scab susceptibility of a diverse Malus germplasm collection identifies potential sources of resistance for apple breeding. CABI Agriculture and Bioscience, 2020;1:1-14.
19. Gygax M, et al. Molecular markers linked to the apple scab resistance gene Vbj derived from Malus baccata jackii. Theoretical and Applied Genetics. 2004;109:1702-09.
20. Joshi SG, et al. Functional analysis and expression profiling of HcrVf1 and HcrVf2 for development of scab resistant cisgenic and intragenic apples. Plant Molecular Biology. 2011;75:579-591.
21. Khajuria, A., et al. "Phenotyping, genetics, and “-omics” approaches to unravel and introgression enhanced resistance against apple scab (*Venturia inaequalis*) in apple cultivars (*Malus × domestica*). *Horticulture Research*. 2024;11(2):uhae002.
22. Patocchi, A., et al. "Rvi4 and Rvi15 are the same apple scab resistance genes.*BMC Plant Biology*. 2023;23(1):505.
23. Parisi, L., et al. "A new race of *Venturia inaequalis* virulent to the Vf gene for scab resistance. *Phytopathology*. 2003;93(4):370-373.
24. Gad, A. F. "Inheritance of Apple (*Malus domestica* (L.) Borkh) Resistance against Apple Scab (*Venturia inaequalis* (Cooke) Wint.) in Hybrid Breeding Material Obtained by Gene Pyramiding. *Horticulturae. 2022;*8(9):772.25. Li Z, et al. Review of deep learning-based methods for non-destructive evaluation of agricultural products. Biosystems Engineering, 2024;245:56-83.
26. Kodors S, et al. Apple scab detection using CNN and Transfer Learning. 2021.
27. Patidar A, Chakravorty A. Using machine learning to identify diseases and perform sorting in apple fruit. International Journal of Innovative Science and Research Technology. 2024.
28. Redmon J, et al. You only look once: Unified, real-time object detection. in Proceedings of the IEEE Conference on Computer Vision and Pattern Recognition. 2016.
29. Alif MAR, Hussain M. YOLOv1 to YOLOv10: a comprehensive review of YOLO variants and their application in the agricultural domain. arXiv Preprint. arXiv:2406.10139, 2024.

30. Rouš R, et al. Apple scab detection in orchards using deep learning on colour and multispectral images. arXiv Preprint. arXiv:2302.08818, 2023.
31. Sikati J, Nouaze J. YOLO-NPK: A Light Deep Network for Lettuce Nutrients Deficiency Classification Based on Improved YOLOv8 Nano. 2023;5:2023.
32. Lu Y, Lu R, Zhang Z. Development and preliminary evaluation of a new apple harvest assist and in-field sorting machine. Applied Engineering in Agriculture. 2022;38(1):23-35.
33. Rath SR. Apple fruit scab recognition using deep learning and PyTorch, in debuggercafe.com. 2022: Debugger Cafe.
34. Kavya P, et al. Deep analysis: apple fruit disease detection using deep learning. 2024 IEEE International Conference on Information Technology, Electronics and Intelligent Communication Systems (ICITEICS). 2024. IEEE.
35. Mahlein A-K. Plant disease detection by imaging sensors–parallels and specific demands for precision agriculture and plant phenotyping. Plant Disease. 2016;100(2):241-51.
36. Weibel FP, Schmid A, Häseli A. Efficient multi-location testing of scab resistant cultivars for organic apple production in Switzerland. XXVI International Horticultural Congress: Genetics and Breeding of Tree Fruits and Nuts. 2002;622.
37. Dwyer B, Nelson J, Hansen T, et. al. Roboflow. 2024;(Version 1.0).
384. Lateur M, Populer C. Screening fruit tree genetic resources in Belgium for disease resistance and other desirable characters. Euphytica. 1994;77:147-53.
39. Rao SN. YOLOv11 Architecture explained: next-level object detection with enhanced speed and accuracy. 2024: Medium.com. p. A brief article all about the recently released YOLOv11 from its architecture to its performance. This is all you want to know about.
40. Keskar NS, et al. On large-batch training for deep learning: Generalization gap and sharp minima. arXiv preprint arXiv:1609.04836, 2016.
41. Khajuria YP, et al. Avirulence (Avr) genes in fungal pathogen Venturia inaequalis, a causal agent of scab disease on apple trees. Physiological and Molecular Plant Pathology. 2023;127:102101.
42. Bleasdale, AJ, Whyatt JD. Classifying early apple scab infections in multispectral imagery using convolutional neural networks. Artificial Intelligence in Agriculture. 2025;15(1):39-51.
43. Laloi G, et al. Efficiency of pyramiding of three quantitative resistance loci to apple scab. Plant Pathology, 2017;66(3):412-22.
44. Liebhard R, et al. Mapping quantitative field resistance against apple scab in a 'Fiesta'×'Discovery' progeny. Phytopathology. 2003;93(4):493-501.
45. Ahmed I, Yadav PK. Predicting apple plant diseases in orchards using machine learning and deep learning algorithms. SN Computer Science. 2024;5(6):700.
46. Mir S, et al. Mapping of quantitative trait loci for scab resistance in apple (Malus× domestica) variety, Shireen. Molecular Biology Reports, 2022;49(6):5555-66.
47. He K, et al. Mask R-CNN. Proceedings of the IEEE international Conference on Computer Vision. 2017.
48. Chu P, et al. Deep learning-based apple detection using a suppression mask R-CNN. Pattern Recognition Letters, 2021;147:206-11.
49. de Melo RF, et al. Diagnosis of apple fruit diseases in the wild with mask R-CNN. in Brazilian Conference on Intelligent Systems. 2020. Springer.
50. Jurewicz M, Świderski B, Kurek J. Application of Mask R-CNN algorithm for apple detection and semantic segmentation. Przeglad Elektrotechniczny. 2024;2024(5).
51. Kirillov A, et al. Segment anything. in Proceedings of the IEEE/CVF international conference on computer vision. 2023.
52. Chiang C, et al. ASPEN study case: real time in situ apples detection and characterization. Smart Agricultural Technology. 2024;8:100506.

53. Nguyen Quoc K, et al. Using the New YoLo models in detecting small-sized objects in the case of rice grains on Branche. International Conference on Data Science and Artificial Intelligence. 2023. Springer.
54. Nouaze JC, Sikati J. YOLO-appleScab: a deep learning approach for efficient and accurate apple scab detection in varied lighting conditions using CARAFE-enhanced YOLOv7. Biology and Life Sciences Forum. 2023. Multidisciplinary Digital Publishing Institute.